Reeves, et al., in Substorms 3, ESA SP-339, 579-584, 1996.

Radial Propagation of Substorm Injections

G. D. Reeves, M. G. Henderson, P. S. McLachlan, and R. D. Belian

Mail Stop D-436, Los Alamos National Laboratory, Los Alamos, NM 87545, USA, email = reeves@lanl.gov

and

R. H. W. Friedel, and A. Korth

Max Planck Institut fur Aeronomie, Katlenburg-Lindau, Germany

ABSTRACT

We report on a study of dispersionless substorm injections. We identified dispersionless substorm injections using CRRES EPAS and LANL geosynchronous energetic particle data. We found 29 substorms for which dispersionless injections could be observed by two spacecraft and we calculated the delay time as a function of the radial separation of the satellites. We found that essentially all cases were consistent with an inward/earthward propagation of the substorm injection region. For 9 of the 29 events the two spacecraft were within ± 1 hour of local time. For those 9 events the delay time was nearly linear with radial separation. The propagation speed calculated from a linear fit to those data was approximately 24 km/s. The earthward propagation of the substorm injection region is basically consistent with the "convection surge" model of substorm injections but does not necessarily contradict the "current disruption" model. The relatively slow apparent velocity of radial propagation is more difficult to reconcile with the expected convection velocities and with the extremely sharp onsets that are observed at both satellites.

1. INTRODUCTION

The injection of energetic particles near the inner edge of the plasma sheet is one of the most common and reliable indicators of substorm onset. Substorm injections are observed at geosynchronous orbit in association with nearly every substorm identified by other means. During the growth phase a decrease of energetic particle fluxes in the midnight sector caused by thinning of the plasma sheet is frequently observed. Within a few minutes of onset the fluxes not only return to their previous levels but, typically, are enhanced by up to several orders of magnitude. The enhancement of energetic particles measured in a particular energy band indicates an energization of the distribution and is referred to as a substorm injection. Substorm injections near geosynchronous orbit are most clearly and most commonly observed at energies of tens to hundreds of keV. When all energies are enhanced (injected) simultaneously it is referred to as a "dispersionless" injection. The region of space in which dispersionless injections are observed is referred to as the "injection region". When a spacecraft is outside the injection region it frequently observes enhancements of energetic particles that have drifted out of the injection region and are therefore observed with a velocity, or energy, dispersion.

Here we are not concerned with the drift of energetic particles out of the injection region. Rather we seek to identify propagation of the injection region itself. We do this by identifying dispersionless injections seen by two satellites in association with a single substorm and by measuring the time delay as a function of radius and local time. Only the radial propagation will be discussed here. The local time propagation is discussed in a more detailed paper [Ref. 1].

Determining the radial propagation of the injection region can help to distinguish among different mechanisms that have been proposed to explain dispersionless substorm injections. Two competing scenarios for substorm injections have been proposed. Figure 1*a* illustrates the "convection surge" mechanism [Ref. 2], [Ref. 3]. In this picture there is a distinct earthward boundary to the substorm injection region but no clear tailward boundary. Rather the boundary is a sharp "injection front" produced by the earthward convection of energized particles. The convection is produced by the inductive electric field associated with the dipolarization of the magnetic field at substorm onset. In this model, at a given magnetic meridian the propagation of the injection region would be earthward. Figure 1*b* is adapted from Lopez & al. [Ref. 4] who re-interpreted the injection boundary as the spatial limit on a region of instability associated with "current disruption". Earthward of the injection boundary the tail is assumed to be stable and tailward of that boundary particles could be energized by one of a variety of instabilities such as the cross-tail current instability or the ballooning instability. In this scenario the injection starts in a small region that is bounded radially (both inward and outward) and azimuthally. It subsequently expands azimuthally and radially tail-

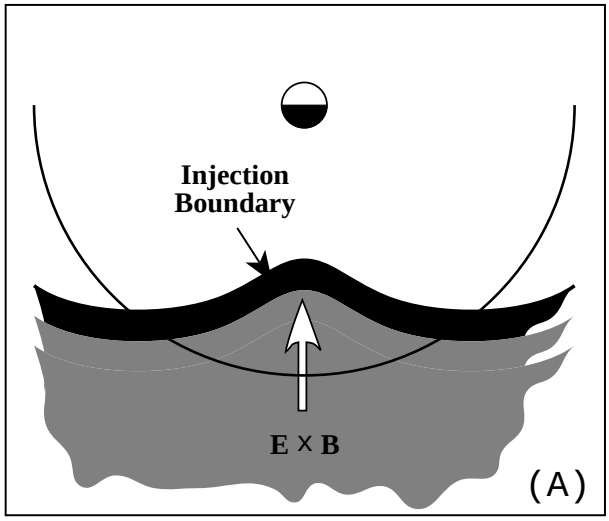

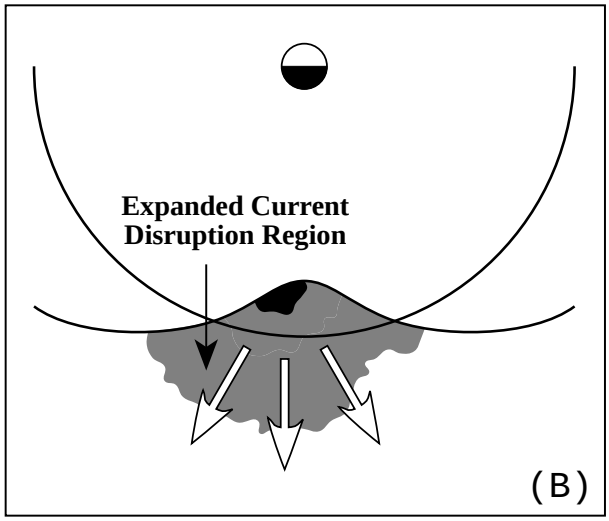

Figure 1: Propagation of the substorm injection region predicted by (A) the Convection Surge model and (B) the Current Disruption model.

ward but is always bounded on the earthward side by the assumed spatial limit on where the instability can operate. In this model the expansion of the injection region does not imply tailward convection of the particles but rather the tailward propagation of the region in which particles are energized. We note also that in the "current disruption" scenario particles are energized locally through an *in situ* instability whereas in the "convection surge" scenario particles might either be energized fairly locally or be energized at a more distant, downtail, location and convected into the region where they are observed.

The two scenarios for the substorm injection mechanism are related to what might be the central controversy in substorm studies, illustrated in Figure 2. The top panel shows a scenario that is normally associated with the Near-Earth Neutral Line model. In this picture substorm onset begins with reconnection in the middle magnetotail (at perhaps 20-30 R_E) and the effects propagate earthward, perhaps through bursty bulk flows. In the bottom panel

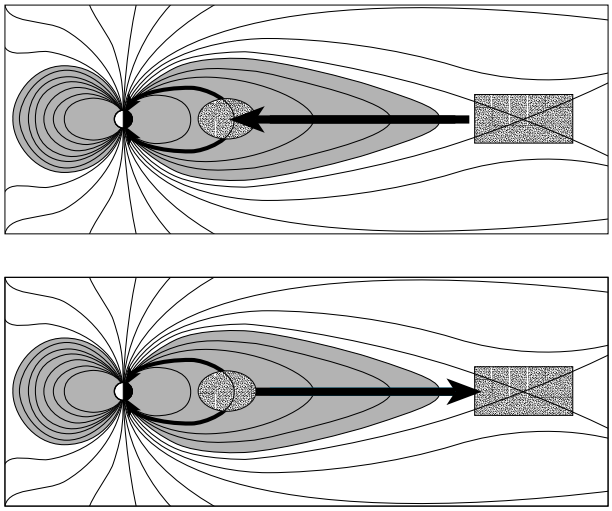

Figure 2: This schematic represents a fundamental controversy in space plasma physics. The Near-Earth Neutral Line model proposes that the substorm initiates in the mid tail at a reconnection site and that the effects subsequently propagate earthward. The Current Disruption model proposes that the substorm initiates near the inner edge of the plasma sheet and that a tailward-propagating rarefaction wave could later produce reconnection in the more distant tail.

the substorm onset occurs in the closed field line region near geosynchronous orbit ($\approx 6 - 10R_E$) and propagates tailward, perhaps through a rarefaction wave which might also cause reconnection in the tail. This general picture is often referred to as the Current Disruption model. Both of these basic scenarios now account for the widely accepted observations of substorm-associated plasmoids in the distant tail (e.g. [Ref. 5]) and of the mapping of auroral processes to the near geosynchronous region (e.g. [Ref. 6], [Ref. 7]). They differ mainly in the relative timing and radial propagation of substorm phenomena.

2. DISPERSIONLESS INJECTIONS AT TWO SATELLITES

In order to determine the propagation direction of substorm injection signatures in the near-earth magnetosphere we compared the onset times of dispersionless injection signatures seen at geosynchronous orbit ($\approx 6.6R_E$) with the onset times seen by the CRRES satellite which was in a geosynchronous transfer orbit and therefore radially earthward of $6.6R_E$. The CRRES data used here were obtained with the EPAS instrument [Ref. 8] which measures electrons with energies from 21 to 285 keV and protons from 37 keV to 3.2 MeV. The geosynchronous energetic particle data were obtained by the Los Alamos National Laboratory CPA and SOPA instruments which also measure protons and electrons with energies above a

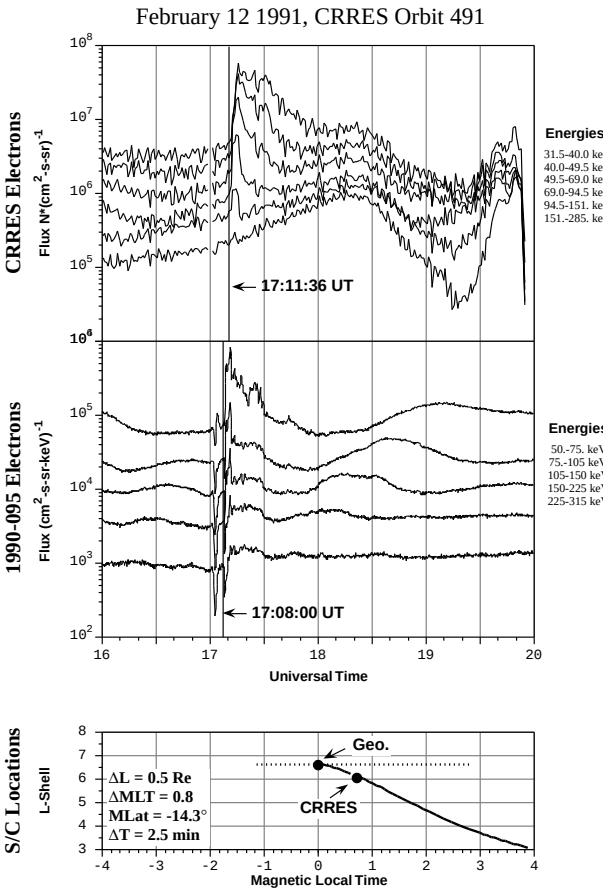

Figure 3: An example of a dispersionless injection seen by CRRES and by LANL geosynchronous satellites. CRRES was located $0.5R_E$ earthward of 1990-095 and observed the injection 2.5 min later.

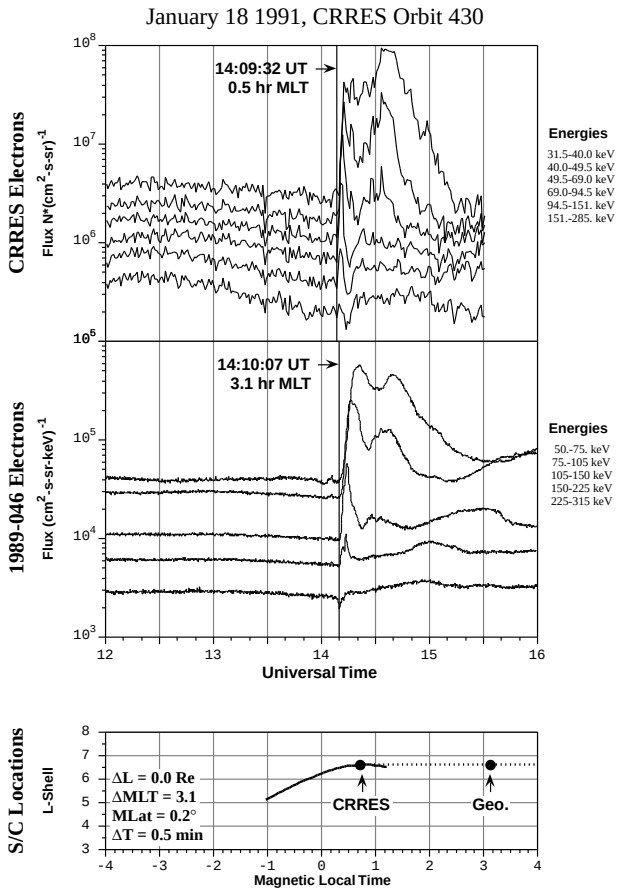

Figure 4: Another example of a dispersionless injection seen by CRRES and by LANL geosynchronous satellites. Both satellites were at $\approx L = 6.6R_E$ but were separated by about 3 hours of local time. Both satellites observed a dispersionless injection at $\approx$ 1410 UT.

few tens of keV. (See [Ref. 9] for more details.)

We began by surveying CRRES summary plots of energetic electron and ion data to identify substorm injections. We then identified the subset of injections that had no energy dispersion, indicating that CRRES was within the injection region. For each of those events we then surveyed the Los Alamos geosynchronous energetic particle data to determine if one of the four available satellites also observed a dispersionless injection.

Figure 3 shows one example of a dispersionless substorm injection that was observed by both CRRES and one of the LANL geosynchronous satellites. The relative locations of the two satellites is shown in the bottom panel. At the time of onset the satellites were separated by $0.5R_E$ and 0.8 hours of MLT. The geosynchronous satellite 1990-095 observed a dispersionless electron injection at 1708:00 UT. CRRES observed a dispersionless electron injection 2.5 min later at 1711:36 UT. The CRRES data used in this study were 1-min averages while the LANL data were 10-s averages. Therefore the uncertainties in the timing of the injection onsets are $\pm$1 min and $\pm$10 s respectively. The 2.5 min delay between the injection times is significant compared to the uncertainties in the timing and we assume that it is due to the spatial separation of the two satellites.

In Figure 3 the flux variations observed by CRRES after 1800 UT are not due to substorm activity. They are a result of the passage of CRRES through the radiation belts along its orbit.

Figure 4 shows another example of a dispersionless substorm injection observed by CRRES and the geosynchronous spacecraft 1989-046. A dispersionless substorm onset was observed at 1410 UT by both spacecraft. At that time both spacecraft were at about $6.6R_E$ but 1989-046 was about 3 hours east of CRRES. To within the uncertainty in the timing of the CRRES onset ($\pm$1 min) both spacecraft observed the injection simultaneously. Furthermore the temporal structure of the injection looks similar at the two satellites – with a double-peaked structure observed at energies below about 150 keV – confirming that substorm injections can sometimes be coherent over a fairly broad range of local times.

3. PROPAGATION STATISTICS

The entire data set available from the CRRES mission was surveyed for events such as that shown in Figure 3. A number of events had to be eliminated from the study because of ambiguous onset times. This was usually caused by the presence of pseudo-breakups or multiple onsets. We identified 29 events for which there were clear, unambiguous, and dispersionless onsets observed by CRRES and by one of the LANL geosynchronous satellites.

For each of those 29 events we calculated the delay between the injection at geosynchronous orbit and the injection seen by CRRES. In Figure 5 the delay times are plotted as a function of the L-shell occupied by CRRES. Negative delay times indicate that CRRES observed the dispersionless injection later than the LANL geosynchronous satellite. When CRRES was at $L < 6.6R_E$ this implies an inward or earthward propagation. Because of its orbit CRRES spent almost all of its time inside geosynchronous orbit.

These results strongly suggest that the most common direction of propagation for the injection region is earthward. The one event that appears to be substantially inconsistent with that trend is unusual in that CRRES was at 23.5° magnetic latitude. At that latitude the calculation of L is quite uncertain. If the magnetic field is more stretched than the model used to calculate L then CRRES could easily have been on a field line that mapped to outside geosynchronous orbit rather than just inside as the model field would indicate.

While the results shown in Figure 5 are consistent with earthward propagation of the injection region they also include the effects of azimuthal separation of the satellites. In order to better asses the effects of radial propagation we plot in Figure 6 only those nine events for which CRRES was within ±1 hr of the LANL geosynchronous satellite. The format of Figure 6 is the same as Figure 5 but the scale is expanded.

Figure 6 also shows the earthward propagation apparent in Figure 5 but much of the scatter in the delay times is removed. This confirms that the scatter in Figure 5 is most likely due to the azimuthal separation of the satellites. More importantly, Figure 6 indicates that there is a systematic relationship between the delay times and the radial separation of the spacecraft. A straight line fit to the data gives a correlation coefficient of 77% and, coincidentally, gives zero delay time for zero radial separation.

The slope of the straight line fit to the data in Figure 6 gives us the average velocity of the propagation of the injection region. That velocity is approximately 24 km/s which means that it takes the injection region about 4.5 minutes to move earthward by $1R_E$

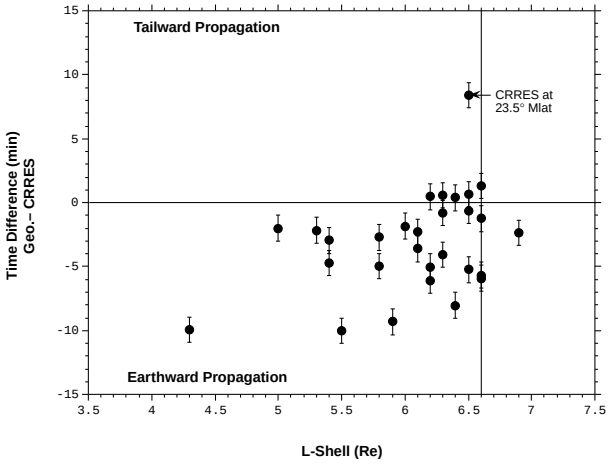

Figure 5: The time delay between dispersionless injections measured at geosynchronous orbit and at CRRES are plotted as a function of the location of CRRES in L for all 29 events in this study. When CRRES is at $L < 6.6R_E$ negative time delays imply earthward propagation.

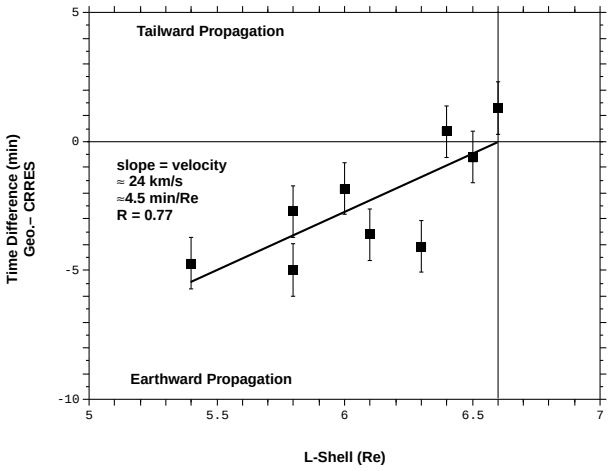

Figure 6: The nine events for which the two spacecraft were within ±1 hr of local time are plotted in the same format as Figure 5. A linear fit to the data gives a very good correlation and implies an earthward propagation velocity of approximately 24 km/s.

4. CONCLUSIONS

We have examined the entire CRRES data set to find events for which we could determine the delay time between dispersionless substorm injections observed by CRRES and by one of the Los Alamos geosynchronous satellites. We found 29 events for which we could calculate the delay time between the onsets of the injections seen at the two satellites. Essentially all of the events that we analyzed were consistent with an inward propagation of the injection region from geosynchronous orbit toward the earth. For the nine events for which the two satellites were separated by less than one hour of local time the delay time was approximately linear with radial separa-

tion.

These observations are completely consistent with the predictions of the convection surge model of substorm injections [Ref. 2], [Ref. 3]. According to that model, particles are energized by the dipolarization of the magnetic field (or possibly some other source) and are convected earthward by the inductive electric field. At first, our results appear to contradict the predictions of the current disruption model which assumes that the region of current disruption propagates tailward along with a magnetic rarefaction wave. We note however that this study only investigates the propagation of the injection region inside geosynchronous orbit. We can assume that the propagation we observe is the propagation of the inner boundary of the injection region. Therefore it is conceivable that the two models are not mutually incompatible. It may be that a current disruption region forms somewhere near or outside geosynchronous orbit and that it generally propagates tailward. At the same time the dipolarization of the magnetic field that is caused by the disruption of current produces an inductive electric field that convects the accelerated particles earthward.

We note however that if injection is caused by an energization of the *in situ* plasma populations by dipolarization of the magnetic field then our results suggest that the dipolarization itself would have to propagate earthward. In that case the propagation speed is the speed of the compressional wave. On the other hand if the particles are accelerated somewhere outside geosynchronous orbit and convected earthward then the propagation speed is the actual convection velocity of the particles.

The second major result of this study is the first calculation of the velocity of the radial propagation of the injection region. Based on a linear fit to the observed delay times as a function of radial separation we calculated that the injection region propagates earthward at approximately 24 km/s.

A velocity of 24 km/s is surprisingly slow. The low velocity of propagation would appear to rule out all but convection as a possibility. However, attributing the radial propagation of the injection region to convection poses several difficulties as well. One problem is quantitative. The inductive electric fields produced by dipolarization of the electric field have been measured to be about 20 mV/m which would produce a convection velocity of several hundred km/s [Ref. 10]. Another problem is the sharpness of the injection onset. If the injection is due to convection then the flux profiles as a function of time can be converted to flux profiles as a function of radius. Therefore a rapid injection of particles implies that there is a very steep gradient at the boundary with higher fluxes of energetic particles tailward of that boundary. A final problem involves the azimuthal drift of the particles while they are being injected. The injection is usually assumed to be very fast so that azimuthal drifts are negligible during the injection. If the injection is slow then higher energy particles would be injected over a larger range of local times than lower energy particles. To our knowledge no observations have been reported that would suggest that this is the case.

Of course our study of delay times between the CRRES and LANL geosynchronous satellites can also be used to investigate the azimuthal propagation of the injection region. Preliminary analysis has not revealed any systematic propagation. However, we are continuing that analysis and will present the results in a future publication.

Finally, we note that our calculated velocity for the radial propagation of the injection region also has implications for the source region of the injected particles. Numerous case studies have shown that dispersionless substorm injections are typically observed within a few minutes of onsets seen on the ground in auroral observations, Pi2 pulsations, and magnetometer data. If we assume that we can extrapolate our calculated velocity to regions just outside geosynchronous orbit then the short delay time between "substorm onset" and "injection onset" at geosynchronous orbit implies that the source region for the injected particles is within a few R_E of geosynchronous orbit. To investigate this possibility more directly we are currently analyzing the propagation of substorm injections in the region outside geosynchronous orbit using data from AMPTE/CCE.

REFERENCES

1. Reeves G D & al 1996, Propagation of the substorm injection region measured by LANL and CRRES, *J. Geophys. Res.*, submitted.

2. Mauk B H & C E McIlwain 1974, Correlation of K_p with the substorm-injected plasma boundary, *J. Geophys. Res.*, 79, 3193.

3. Moore T E & al 1981, Propagating substorm injection fronts, *J. Geophys. Res.*, 86, 6713.

4. Lopez R E & al 1990, The energetic ion substorm injection boundary, *J. Geophys. Res.*, 95, 109.

5. Slavin J A & al 1990, IMP-8 observations of traveling compression regions: New evidence for near-earth plasmoids and neutral lines, *Geophys. Res. Lett.*, 17, 913.

6. Elphinstone R D & al 1991, Mapping using the Tsyganenko long magnetospheric model and its relationship to Viking auroral images, *J. Geophys. Res.*, 96, 1467.

7. Reeves G D & al 1996, Quantitative experimental verification of the magnetic conjugacy of geosynchronous orbit and the auroral zone, in *Proceedings of the third international conference on substorms (ICS-3)*, this volume.

8. Korth A & al 1992, Electron and proton wide-angle spectrometer (EPAS) on the CRRES spacecraft, *J. Spacecr. Rockets*, 29, 609.

9. Reeves G D & al 1996, Los alamos space weather data products: On line and on time, in *Proceedings of the third international conference on substorms (ICS-3)*, this volume.

10. Aggson T L & al 1983, Observations of large magnetospheric electric fields during the onset phase of a substorm, *J. Geophys. Res.*, 88, 3981.